

See discussions, stats, and author profiles for this publication at: <https://www.researchgate.net/publication/281370153>

The Properties of Phenol Confined in Realistic Carbon Micropore Model – Experiment and Simulation

ARTICLE *in* THE JOURNAL OF PHYSICAL CHEMISTRY C · AUGUST 2015

Impact Factor: 4.77 · DOI: 10.1021/acs.jpcc.5b06136

CITATION

1

READS

45

5 AUTHORS, INCLUDING:



[Sylwester Furmaniak](#)

Nicolaus Copernicus University

117 PUBLICATIONS 846 CITATIONS

SEE PROFILE



[Piotr A Gauden](#)

Nicolaus Copernicus University

224 PUBLICATIONS 1,943 CITATIONS

SEE PROFILE

Properties of Phenol Confined in Realistic Carbon Micropore Model: Experiment and Simulation

Marek Wiśniewski,^{†,‡} Sylwester Furmaniak,[†] Artur P. Terzyk,^{*,†} Piotr A. Gauden,[†] and Piotr Kowalczyk[§]

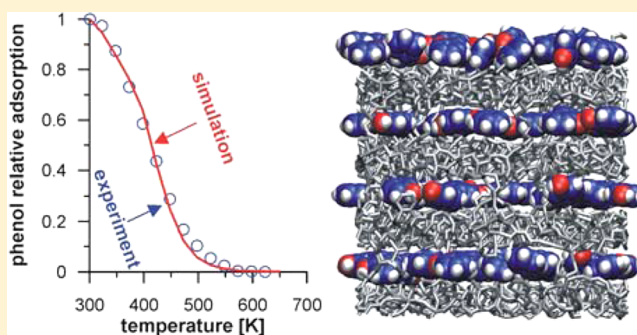
[†]Faculty of Chemistry, Physicochemistry of Carbon Materials Research Group, Nicolaus Copernicus University in Toruń, Gagarin Street 7, 87-100 Toruń, Poland

[‡]R&D Center, INVEST-TECH, 32-34 Plaska St., 87-100 Toruń, Poland

[§]School of Engineering and Information Technology, Murdoch University, Murdoch 6150 WA, Australia

S Supporting Information

ABSTRACT: Adsorption of phenol is still the subject of the never ending debate in the literature. In the current study the results of experimental measurements of phenol adsorption from gas phase on microporous carbon with known atomistic structure are reported for the first time. This structure was reproduced recently using the new reconstruction method proposed in this journal [*J. Phys. Chem. C* **2014**, *118*, 12996–13007]. Next, using the GCMC simulation, we simulate phenol adsorption and we compare simulation with experimental data. The comparison of behavior of phenol in realistic pores with the behavior in ideal slit-like pores is given. The discussion leads to interesting conclusions about the value of k factor and about the properties of adsorbed phenol (RDF, number of hydrogen bonds, etc.). To our knowledge, this is the first paper showing the behavior of phenol in pores of realistic carbon.



1. INTRODUCTION

Phenol is the most widely studied pollutant. Its anthropogenic origin in the environment is due to the activity of the chemical, petrol, tinctorial, or pharmaceutical industries (see for example ref 1). Moreover, phenols stem from the production and use of numerous pesticides.^{2,3} Activated carbons are still widely used in different processes of water purification, and adsorption on commercial activated carbons is an important stage in water treatment plants. This is caused not only by strong affinity of phenol to carbon (and large adsorption capacity) but also by the properties of carbon, allowing the growth of phenol-consuming bacteria in pores.^{4–6} At the same time, the hydrophobic nature of carbon surface causes relatively low affinity toward the most common solvent—water. Different mechanisms of phenol adsorption have been proposed (see ref 7 and references therein). However, in our opinion, to understand the mechanism of phenol adsorption in carbon pores on the microscopic level, one should overcome different difficulties. First of all, the detailed structure of carbon pores (pore walls) is still unknown, and at the present authors usually assume slit-like pores. This is probably true if we consider the graphitizable (i.e., “soft”) carbon. However, in the case of so-called “hard” carbons, we know that pore walls are probably built of curved graphene sheets, preserving graphitization. The presence of curved sheets was proposed by Harris et al.^{8–10} on the basis of HRTEM studies of nongraphitizing carbons. To overcome this problem, and to reconstruct carbon structure, one can use recently developed methods.^{11–15} One recently

reported by us is a procedure based on hybrid reverse Monte Carlo simulation.¹⁶ Application of this procedure coupled with wide-angle X-ray scattering experiments was used for constructing an atomistic level model of a representative sample of carbon film synthesized in our laboratory. We found that this material possesses a disordered matrix enriched with bended carbon chains and various carbon clusters as opposed to the turbostratic carbon or graphite-like microcrystals. The pore structure of this film has a defected lamellar morphology of one-dimensional periodicity with narrow (ca. 0.4 nm) micropores. On the other hand, to evaluate the behavior of phenol in such a realistic pore model, one should compare the results of simulation with experimental data. We still do not know exactly to what extent different hybridizations of carbon atoms forming pore walls change the values of interaction energy parameters. The same can be stated about the presence of solvent. Preliminary simulation data show that the so-called “solvent” effect^{17,18} plays an important role in pore blocking.¹⁹ However, the role of solvent depends not only on the type of surface groups attached to carbon but also on the location of groups. All those factors make the mechanism of organics adsorption from aqueous solutions very complicated. Thus, in our opinion, it is necessary to start the complex study on the mechanism of phenol adsorption from solution. A good starting

Received: June 26, 2015

Revised: August 11, 2015

Published: August 11, 2015

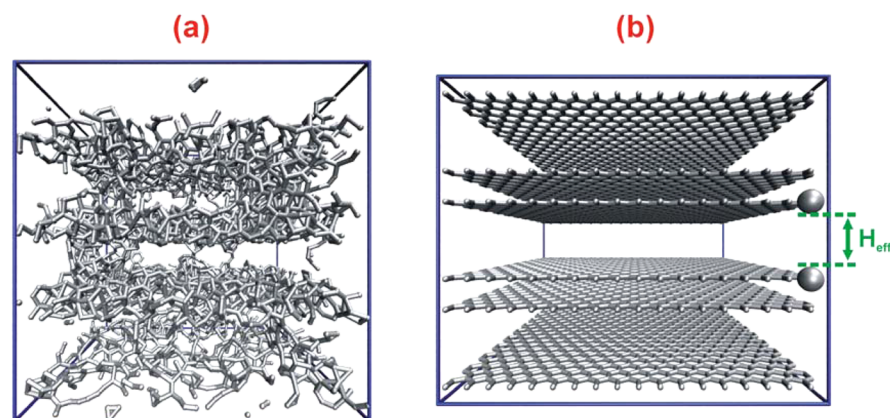


Figure 1. Schematic representation of the structure of (a) the replica of considered material and (b) model slit-like system. The frames reflect the size of simulation box. It should be noted that this figure and all the animations were created using the VMD program.³²

point is the study on the behavior of phenol adsorbed from the gas phase on realistic carbon model. Since the isotherms of phenol adsorbed from aqueous solutions on carbons are usually of H type following the classification of Giles et al.,^{20,21} the behavior of phenol adsorbed from gaseous phase can be close to the behavior of phenol adsorbed from concentrated solutions. To study this behavior, we use molecular simulation of phenol adsorption on developed recently realistic carbon model. The results of simulation are compared with the experimental data of phenol adsorption from gaseous phase. Bertoncini et al.²² studied, using the GCMC method, the behavior of phenol adsorbed in amorphous carbon pores. They concluded that phenol adsorbed in pores (298 K) is a quasi-solid having approximately 3 times larger density than phenol adsorbed on an open surface. The same group studied the properties of phenol adsorbed on graphite.²³ In the range of temperatures 250–350 K phenol interactions with surface are too weak to form an ordered structure. The enthalpy of adsorption at zero coverage was estimated as equal to -35 kJ/mol, and the phenol cross-sectional area was equal to 0.485 nm².

To our knowledge, probably due to low phenol vapor pressure, experimental gas adsorption data measured for phenol on activated carbon were reported only once in the paper published by Stoekli and Hugi-Cleary.²⁴ They concluded that phenol adsorption mechanism from gas phase follows the mechanism of the pore filling, and the molar volume of adsorbed phenol is ca. 90 cm³/mol. Thus, the major purpose of the present study is to perform the molecular simulation of phenol adsorption in the pores of realistic carbon model, obtained previously from reverse Monte Carlo simulation.¹⁶ Next we compare the data with the experiment and we modify the values of interaction parameters to make the fit to experimental data as good as possible. Finally, we compare the state of phenol in realistic micropores with the same observed in slit-like micropores. The analysis provides the number of created hydrogen bonds, the radial distribution functions of adsorbed molecules, etc.

2. EXPERIMENTAL METHODS

Carbon films used in this study were prepared from cellulose. The charring experiments were described in detail elsewhere.^{16,25–27} The cellulose films carbonized at 573 K in air for 1 h were evacuated at 873 K for 1 h under the dynamic vacuum (0.13 Pa) to remove surface oxygen. The full structural

characteristics of the tested adsorbent have been described previously.^{16,28,29} Briefly, based on the results of low-temperature nitrogen adsorption, tested carbon film can be regarded as microporous solid with BET surface area close to ca. 480 m²/g.

Phenol adsorption was performed under isobaric conditions ($p = 59$ Pa) changing the temperature of the process from 623 K down to 301 K, with a period of 3 h at each temperature in order to be sure that the equilibrium was achieved. The infrared (IR) spectroscopic studies were carried out in a vacuum cell described previously.^{25–27} The construction of this cell enables the thermal treatment of the carbon film up to 1200 K in any controlled atmosphere or in a vacuum. The IR spectra for the samples were recorded (using Mattson Genesis II) at adsorption temperature, i.e., without cooling down to room temperature. Spectral changes accompanying adsorption of phenol were established by comparing IR spectra of the same film recorded in a vacuum and those recorded under a definite adsorption temperature. The respective gas phase was the background for each carbon film spectrum. This simple operation enables observation of spectral changes of surface, without perturbation from the gas phase.

Once the equilibrium was reached, the band at 1222 cm⁻¹ was integrated (I) and used for further comparison with the *in silico* results. Experimental results were presented as I/I_{max} , where I_{max} is the band of maximum intensity taken at the lowest temperature. The I/I_{max} value represents the experimental value of relative adsorption.

3. SIMULATION DETAILS

For the simulations we use the replica of the considered carbonaceous material generated previously using the hybrid reverse Monte Carlo method—for details see our previous work.¹⁶ It was shown that this replica can be successfully applied to the simulation of isotherms and the enthalpy of adsorption from gaseous phase.¹⁶ The model structure (presented in Figure 1a) is placed in the cubic simulation box having the size $4.0 \times 4.0 \times 4.0$ nm with periodic boundary conditions in all three directions. Porosity of the considered system is characterized by a geometrical method proposed by Bhattacharya and Gubbins (BG).³⁰ The implementation of the method was described in detail elsewhere.³¹ The BG method makes it possible to determine the histogram of pore sizes (i.e., the probabilities of finding the pores having the given effective diameter (d_{eff}) — $P(d_{\text{eff}})$). We also compute the volume of pores accessible for adsorbed molecule (V_{acc}) using the

combination of Monte Carlo integration and the BG method (only the volume of pores having effective diameter above assuming lower limit ($d_{\text{acc,min}}$) is integrated).³¹ We assume different values of $d_{\text{acc,min}}$ (from 0.30 to 0.40 nm with the step of 0.01 nm). The V_{acc} are used to calculate mole volume of adsorbed phenol.

The phenol adsorption isobar (for $p = 59$ Pa, i.e., the saturated $\text{C}_6\text{H}_5\text{OH}$ vapor pressure at 301 K) is simulated using the hyper parallel tempering Monte Carlo (HPTMC) method proposed by Yan and de Pablo.³³ This technique is capable of overcoming the large free energy barrier, and it is also capable of relaxing the system much faster than traditional grand canonical ensemble simulations.³³ The simulation scheme is analogous to what was done in our previous work.^{34,35} We consider 15 replicas for different temperature values (corresponding with the experimental points and additionally 650 K). The HPTMC simulations utilizes 5×10^6 cycles (1 cycle = 100 attempts of the change of each replica state by (i) creation, (ii) annihilation, or (iii) rotation and/or displacement of a randomly chosen molecule with equal probabilities, and one attempt of a configuration swap between a pair of randomly chosen replicas). The first 1×10^6 cycles are discarded to guarantee equilibration.

During the simulations both the carbonaceous structure and the phenol molecules are treated as the rigid ones. $\text{C}_6\text{H}_5\text{OH}$ molecules are modeled using the parameters proposed by Mooney et al.³⁶ This force field reproduces quite well bulk and structural properties such as density, heat of vaporization, and static dielectric constant, etc., of phenol. Also, structural properties (for example RDFs) illustrate the hydrogen bonding nature of phenol and the overall preference for the nearest-neighbor phenols to arrange themselves in a T-shaped pattern about their respective O–H groups.³⁶

The interaction energy between molecule pairs was calculated as the sum of dispersive and electrostatic interactions between pairs of centers. The dispersive interactions are modeled using Lennard-Jones potential.³⁷ Cut-offs are realized by the switching function in a quintic form.³⁸ The energy of electrostatic interactions is calculated using the potential proposed by Fennel and Gezelter.³⁹ The approach proposed by these authors is a simple alternative to the Ewald summation.³⁹ The details of calculations are given in the Supporting Information. Table 1 collects all the values of parameters applied in simulations. Cross-interaction parameters are calculated using the Lorentz–Berthelot mixing rules:³⁷

$$\sigma_{ij} = \frac{\sigma_{ii} + \sigma_{jj}}{2} \quad (1)$$

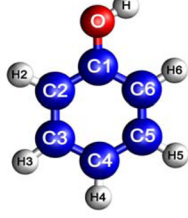
$$\epsilon_{ij} = \sqrt{\epsilon_{ii}\epsilon_{jj}} \quad (2)$$

Since the structure of our carbon replica is far from ideal graphite, one can expect that the parameters for dispersion interaction of C atoms also differ from proposed by Steele⁴⁰ for “flat” carbon surface. In order to fit the simulated phenol adsorption isobar to the experimentally measured one, we modify the value of the potential well depth for C atoms in adsorbent (ϵ_{CC}). This value is increased according to the equation

$$\epsilon_{\text{CC}}^* = k \times \epsilon_{\text{CC}} \quad (3)$$

where k is the scaling factor. We check the following values of k : 1.0, 1.1, 1.2, 1.3, 1.4, 1.5, 1.6, 1.7, 1.8, 1.9, and 2.0. The rise in

Table 1. Values of LJ Potential Parameters and Point Charges Applied in Simulations

	centre	σ [nm]	ϵ/k_B [K]	q/e	Reference
 phenol molecule	C1	0.355	35.36	+0.5400	36
	C2/C6	0.355	35.36	−0.4125	
	C3/C5	0.355	35.36	−0.0300	
	C4	0.355	35.36	−0.3000	
	H2/H6	0.242	15.15	+0.2000	
	H3/H5	0.242	15.15	+0.1430	
	H4	0.242	15.15	+0.1590	
	O	0.307	78.18	−0.6400	
	H	0.000	0.00	+0.4400	
carbonaceous structure	C	0.340	28.00*	—	40

* Starting value.

energetic parameters for adsorbent atoms causes the increase in the solid–fluid interaction energy. According to eq 3 for given k value, the energy is increased by \sqrt{k} . We do not modify the value of collision diameter (σ_{CC}) since it is related to the diameter of carbon atom. The quality of simulated isobar fit to the experimental one is characterized by the determination coefficient:

$$\text{DC} = 1 - \frac{\sum_i (a_i/a_{\text{max}} - I_i/I_{\text{max}})^2}{\sum_i (I_i/I_{\text{max}} - \bar{I}/I_{\text{max}})^2} \quad (4)$$

where a_i/a_{max} and I_i/I_{max} are the simulated and experimental values of relative adsorption for the i th point (in the case of the second value it is equal to the relative intensity) and \bar{I}/I_{max} denotes the average experimental value.

Additionally, we perform phenol adsorption simulations for ideal slit-like pores. We consider the multiplied slit systems (with periodic boundary condition in all three directions) constructed from graphene sheets (4.3959×4.23 nm). Each wall includes two such layers in the distance 0.335 nm. We consider the following effective slit widths (H_{eff}): 0.35, 0.40, 0.45, 0.50, 0.55, 0.60, 0.70, 0.80, 0.90, 1.00, 1.25, 1.50, and 2.00 nm. Each system consists of three slits (see Figure 1b) with exception of $H_{\text{eff}} = 1.50$ and 2.00 nm (for these widths two slits were sufficient to obtain a box size larger than twice of r_{cut} value). In the case of simulation for all slit-like systems we apply the original parameters proposed by Steele⁴⁰ for the flat carbonaceous structures (see Table 1).

In order to analyze equilibrium configurations, we generate 10 000 such configurations for each point on the isobar. We consider the replica for $k = 1.7$ and, additionally, the ideal slit-like systems. We start from the final configuration for each replica, and simulation is continued according to the scheme described previously and actual configurations from the end of each tenth cycle is collected. On the basis of these configurations, we calculate (averaging over all of them) radial distribution functions (RDF, $g(r)$). We analyze the distances between centers of rings in phenol molecules and between oxygen atoms. We also investigate the formation of hydrogen bonds. The average number of them ($\langle n_{\text{hb}} \rangle$) is determined according to the criteria proposed by Gordillo and Martí.⁴¹ Finally, in order to study the location of the center of the benzene rings in phenol molecules inside the slits, we calculate

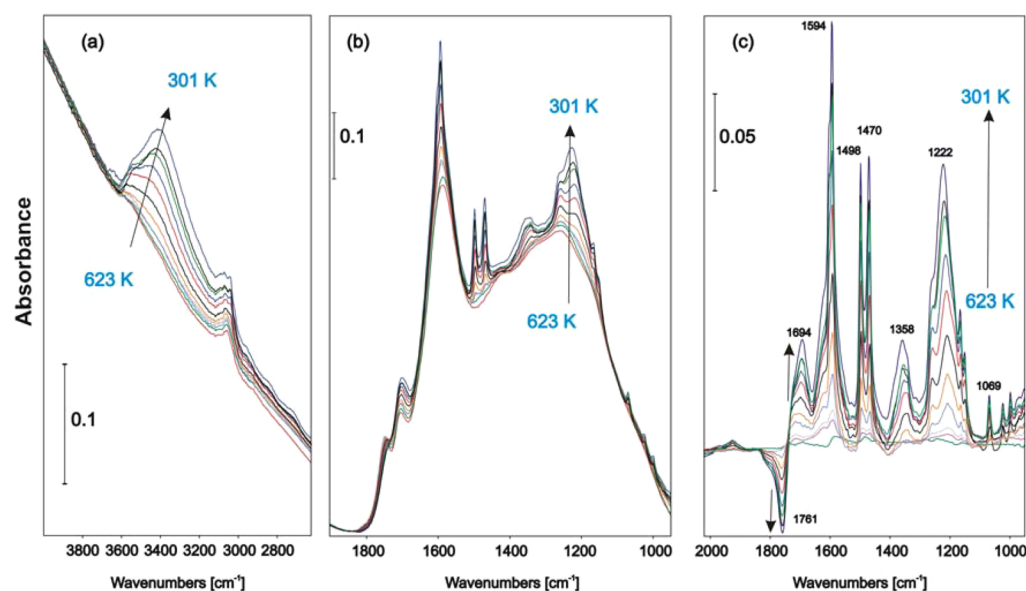


Figure 2. (a, b) FTIR spectra recorded after exposure of carbon film to phenol ($p = 59$ Pa) at temperature range 623 down to 301 K. (c) Differential spectra of the adsorption process (note that IR spectrum of the sample outgassed at 823 K was subtracted).

the density profiles (averaged over all the slits in the system) assuming that location of C_6H_5OH is determined by the ring center.

4. RESULTS AND DISCUSSION

4.1. IR Studies. Figure 2 shows the infrared spectra obtained after exposing studied carbon sample to phenol vapors at decreasing temperatures. Only a few studies⁴² have established the relation between the state of adsorption sites and the wavenumber of adsorbed phenol molecules; however, the process was carried out from water solution. Under isobaric conditions, the decrease in the adsorption temperature causes continuous increase in the intensities of bands observed for physically adsorbed phenol. The occurrence of physical adsorption of phenol is in good agreement with the results of our previous reports.^{43,44} Thus, adsorption process is reversible, and the regeneration of the adsorbent is easy.

The effects of adsorption of the vapors on oxygen-containing, particularly carbonyl, groups present in the carbon films (1761 cm^{-1}) are visible as a couple of negative–positive spectral changes in the $C=O$ region (Figure 2c). However, taking into consideration the total mass content of oxygen in the material (1 wt %), the observed effect is negligibly small. This is why in our model we neglect the presence of heteroatoms.

Some interesting features are observed in the O–H stretching absorptions after phenol vapor exposure. The equatorial –OH group appears here, as a typical polymeric, hydrogen bonded clusters, as a broad band near 3400 cm^{-1} . A smaller peak at higher frequency (3654 cm^{-1}), present already at 301 K, is presumed due to less associated molecules. It means that adsorption mechanism is influenced by the properties of the functional group on the aromatic adsorbate, especially its ability to hydrogen-bond formation and through its activating/deactivating influence on the aromatic ring.

4.2. Fitting Simulation to Experiment. Figure 3 presents the histogram of pore sizes calculated for studied carbon replica using the BG method. The majority of pores of studied carbon are located in the range 0.3–0.5 nm. This result is in good agreement with our previous reports (see for example ref 28).

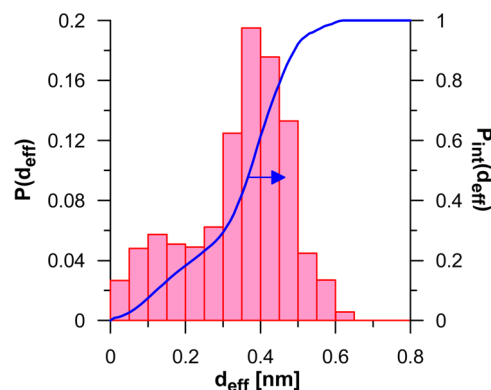


Figure 3. Histogram of pore sizes with resolution of 0.05 nm ($P(d_{\text{eff}})$, bars) and related integral curve with resolution of 0.01 nm ($P_{\text{int}}(d_{\text{eff}})$, line) for the considered replica obtained from the BG method. The $P_{\text{int}}(d_{\text{eff}})$ value shows what part of the pores has diameter up to d_{eff} .³¹

Figure 4a shows determined experimentally (points) and simulated (lines) phenol adsorption isobar curves. As one can see, the application of original sets of interaction parameters ($k = 1$) leads to smaller adsorption values than determined experimentally. Thus, it was necessary to use eq 3 and to simulate additional isobar curves for k in the range $1 < k \leq 2$. Note that a similar procedure was applied by Nguyen et al.⁴⁵ for the estimation of C–C potential energy depth during simulation of hydrogen adsorption isotherm on active carbon. Nguyen et al.⁴⁵ achieved a good agreement between simulated (on carbon replica) and experimental adsorption isotherms. However, this agreement is obtained if the potential well depth for adsorbent atoms is multiplied by the factor 1.33 ($k = 1.33$ according to eq 3). They also provide a possible explanation of this effect. In their opinion the change of carbon surface atom polarizability occurs. From Figures 4b and 4c one can observe that the rise (and next decrease) in DC value is seen with the rise in k value. Moreover, for the best k value simulated data are slightly too large for lower temperatures and are slightly too small for the larger ones (the threshold is located around ca. 400 K). In our case the best fit is observed for $k = 1.7$, and as

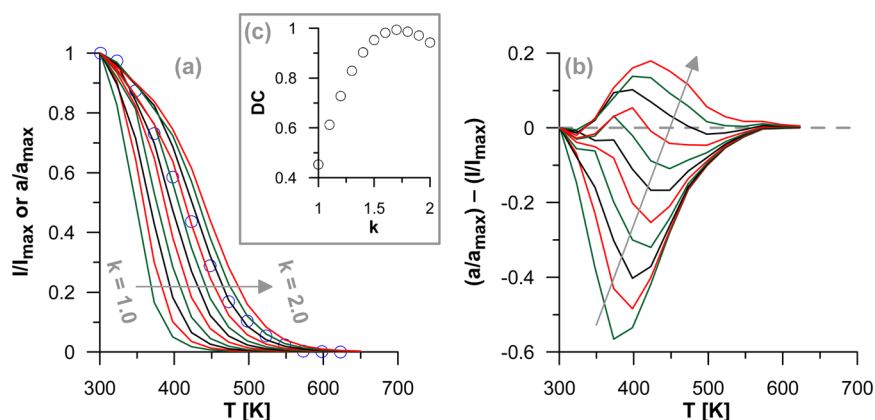


Figure 4. (a) Comparison of experimental phenol adsorption isobar (points) and the data simulated for the replica assuming different values of scaling factor (k) for potential well depth of atoms forming carbonaceous structure (lines). (b) Differences in relative adsorption between the experimental isobar and simulated ones. (c) Calculated values of determination coefficient (eq 4). The arrows show the direction of changes with the rise in k value.

one can see from Figure 5, simulated curve fits very well to the experimental one (DC = 0.9939). The k value is higher than in

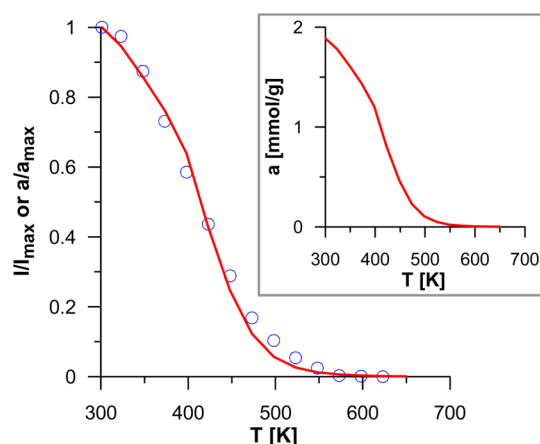


Figure 5. Comparison of experimental phenol adsorption isobar (points) with the best fitted simulated one, i.e., for $k = 1.7$ (line). In addition, the inset presents the absolute adsorption amount obtained from simulations in this system.

the case of Nguyen et al.⁴⁵ This may be caused by the differences in the nature of the considered adsorbents and/or adsorbates. According to eq 2, the obtained k value (equal to 1.7) leads to the increase of the solid–fluid interaction energy value by the factor 1.3.

4.3. State of Phenol in Micropores of Realistic Carbon Model. Figure 6 collects the RDF functions of adsorbed phenol. With the rise in temperature one can observe the progressive changes from quasi-solid to liquid. To obtain more information, we check the number of hydrogen bonds per adsorbed molecule (Figure 7). Animation_01 in the Supporting Information shows equilibrium configurations of adsorbed phenol molecules, and one can observe the creation of hydrogen-bonded clusters confirmed by IR spectra (shown in Figure 2). As it was shown by Mooney et al.,³⁶ the average number of hydrogen bonds created by phenol molecules in melting phenol is close to 0.8 per molecule (a half of the number of first hydrogen bonding groups). In carbon pores this number decreases from 0.5 even down to 0 around 500 K (Figure 7). This is caused by the creation of only one layer

(monolayer) in pores (steric effect). The next effect leading to this decrease in the number of hydrogen bonds is due to orientation of adsorbed molecules. This is influenced by the adsorbate–adsorbent interactions with amorphous carbon atoms forming pore walls. If we compare the results of our experiment with the curves simulated for ideal slit-like pores (Figure 8), one can observe the effect of pore walls heterogeneity on adsorption value. It should be mentioned that there is one irregularity observed for isotherm determined for slit with $H_{\text{eff}} = 0.6$ (marked by a dashed line). The explanation of this behavior is given below. One can see that there are huge differences between the shapes for curves simulated for the slit-like pores and the experimental isobar determined for the studied carbon. Simultaneously, maximum adsorption increases almost linearly with the pore diameter (Figure 8). There are also differences in the behavior of adsorbed molecules. The first peak on ring center–ring center RDF (Figure 9) progressively shifts toward smaller values in slits with the rise in effective pore diameter. In studied carbon (Figure 6) it remains almost at the same position with the rise in T . Moreover, in slit-like pores a larger number of hydrogen bonds per adsorbed molecule are created (see Figure 10) than in the realistic pore model studied in this paper. Animation_02 in Supporting Information shows the comparison of equilibrium configurations of phenol adsorbed in ideal slit-like pores ($H_{\text{eff}} = 0.4$ – 0.5 nm) and in studied carbon pores. This movie confirms given above explanations why the number of hydrogen-bonded molecules in slit-like pores is larger than in carbon replica (note that for a slit with $H_{\text{eff}} = 0.6$ nm the number of hydrogen bonds decreases; see below). In Figure 11 we collect the comparison of density profiles of molecules adsorbed in slit like pores. The profiles as well as the equilibrium configurations presented in animation_03 in Supporting Information explain the behavior of isotherm for the slit having $H_{\text{eff}} = 0.6$ nm. In this movie we compare the molecules adsorbed in ideal slits with $H_{\text{eff}} = 0.5$, 0.6 , and 0.7 nm. Molecules marked using cyan color are at the distance between the center of benzene ring and carbon atoms forming pore walls (the distance to the plane defined by the mass centers of C atoms, i.e., not effective one) larger than 0.45 nm. One can conclude that for slit having $H_{\text{eff}} = 0.5$ nm a monolayer of adsorbed molecules is formed (all the molecules are located at the distance below 0.45 nm), and only some of them have a

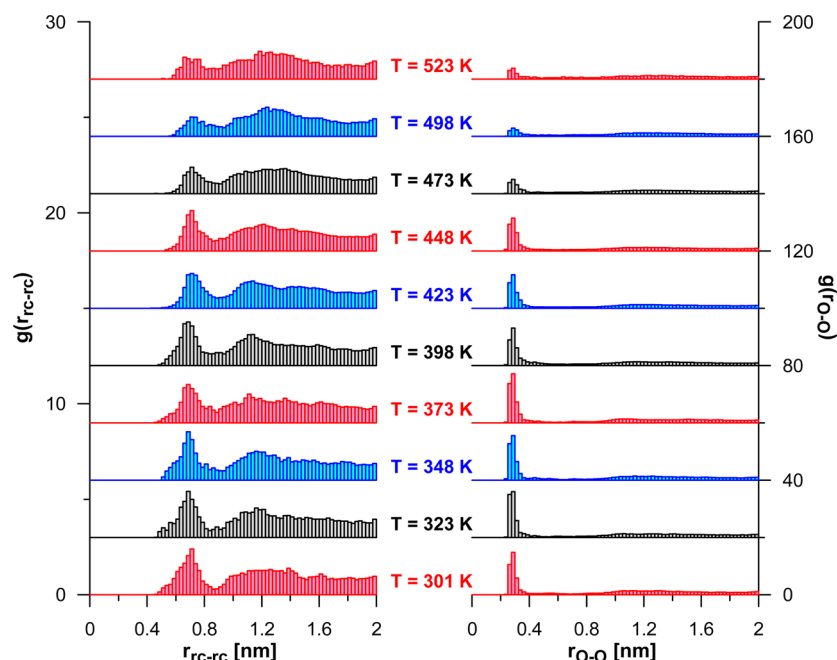


Figure 6. Comparison of ring center–ring center (rc–rc, left) and oxygen–oxygen (O–O, right) RDFs for the selected temperature values calculated for simulated adsorption in the replica for $k = 1.7$. The subsequent RDFs are shifted by 3 (left) and 20 (right) from the previous ones.

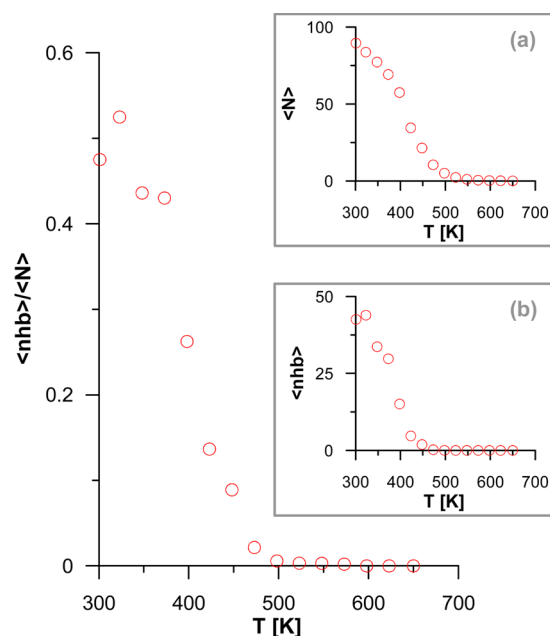


Figure 7. Changes in average number of hydrogen bonds per one phenol molecule with the rise in temperature for the considered replica and $k = 1.7$. In addition, the insets present the average number of phenol molecules in the simulation box $\langle N \rangle$ (a) and the average total number of hydrogen bonds $\langle nhb \rangle$ (b).

nonplanar orientation. The comparison of orientation of molecules adsorbed in pores having $H_{\text{eff}} = 0.6$ and 0.7 nm leads to conclusion that for the larger pore a majority of molecules has flat orientation on pore walls (two layers are created) and small number of molecules has angular orientation. For the smaller considered pore ($H_{\text{eff}} = 0.6$ nm) only some molecules lay on pore walls (only one layer is formed due to small pore diameter), but a majority of molecules have angular orientation. This orientation enables

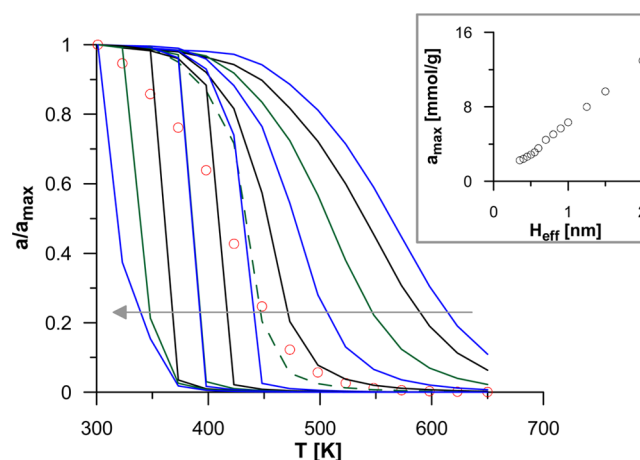


Figure 8. Comparison of phenol adsorption isobars simulated for ideal slit-like systems having different effective width H_{eff} (lines) and for the replica with $k = 1.7$ (points). The arrow shows the direction of changes connected with the rise in H_{eff} value. The data for the system having $H_{\text{eff}} = 0.6$ nm are shown as the dashed line. In addition, the inset shows the maximum adsorption amount (a_{max}) for different systems.

the creation of hydrogen bonds, explaining the anomalous behavior observed in the plots of adsorption isotherms (Figure 8) and the plots of the number of formed hydrogen bonds (Figure 10).

Finally, the molar volume of phenol adsorbed in the replica ($k = 1.7$) at $T = 301$ K was calculated assuming different minimum effective diameters of accessible pores ($d_{\text{acc,min}}$) during volume integration. The results are shown in Figure 12. Observed molar volumes of phenol are reasonable. The value experimentally estimated by Stoeckli and Hugi-Cleary²⁴ (ca. $90 \text{ cm}^3/\text{mol}$) can be observed in our carbon replica if we assume that the minimum pore diameter, accessible for phenol molecules, is equal to 0.37 nm. This corresponds very well

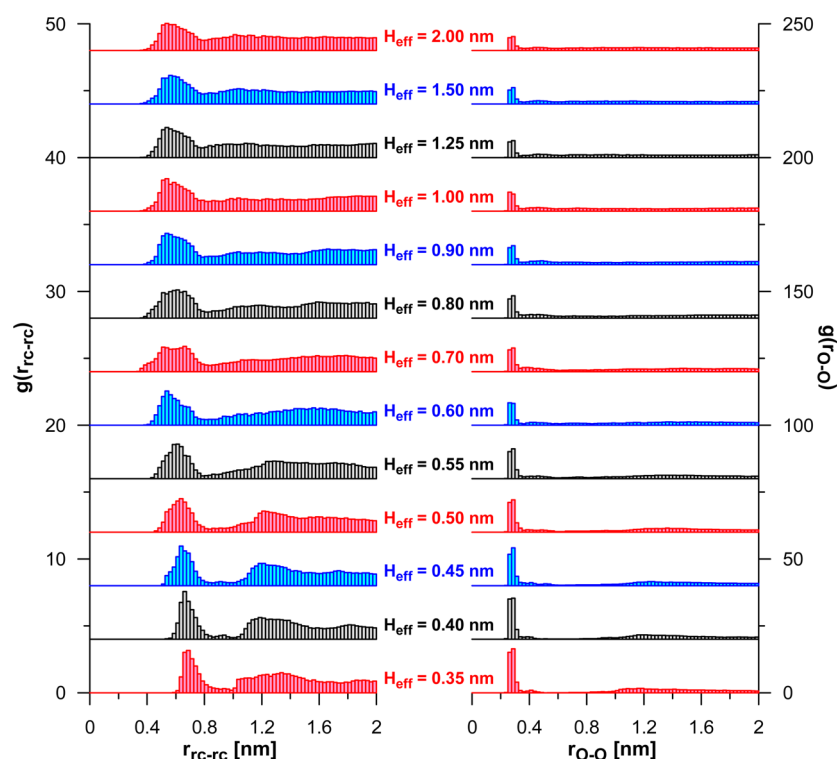


Figure 9. Comparison of ring center–ring center (rc–rc, left) and oxygen–oxygen (O–O, right) RDFs for the all the considered slit-like systems at $T = 301$ K. The subsequent RDFs are shifted by 4 (left) and 20 (right) from the previous ones.

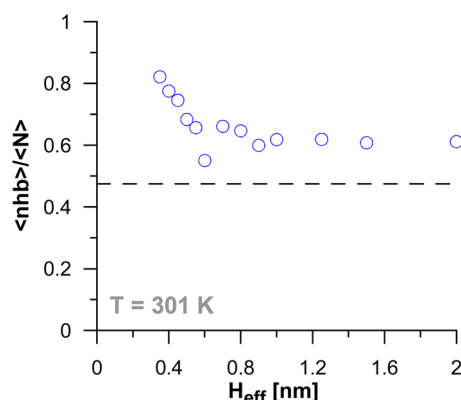


Figure 10. Average number of hydrogen bond per one phenol molecule formed in ideal slit-like systems at $T = 301$ K. For comparison, the dashed line represents the number of hydrogen bonds in replica with $k = 1.7$.

with previous MD simulation results of phenol adsorption on porous carbon models (see Figure 4 in ref 17).

5. CONCLUSIONS

Phenol adsorption simulation results on the replica of microporous carbon are presented for the first time. The comparison with experimental results measured for this carbon shows that the energetic parameters applied in simulations for studied heterogeneous carbon structure should be increased in comparison to those for “flat” carbon structures. The application of modified (using eq 3) parameters leads to excellent agreement between simulated and experimental data.

Because of narrow pores in studied carbon, we observe the creation of mainly monolayer in pores. The average number of hydrogen bonds formed between molecules in this layer is

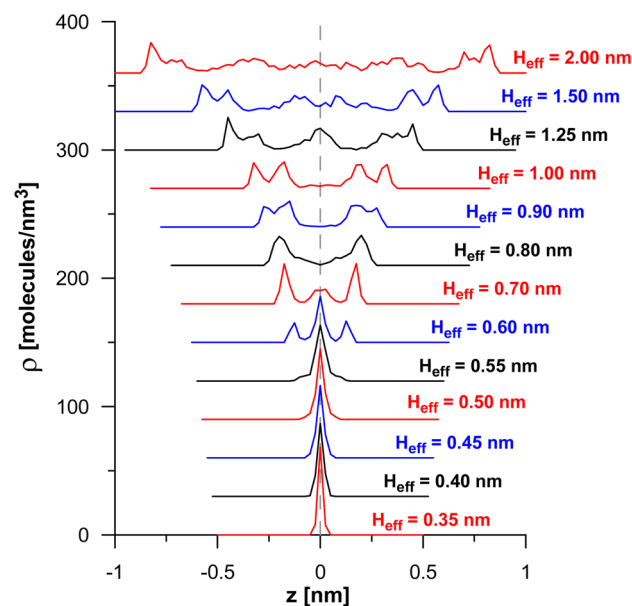


Figure 11. Comparison of location of benzene ring center in slits (density profiles assuming that location of phenol molecules is determined by the ring center). The subsequent curves are shifted by 30 from the previous ones. The data averaged over all the slits in the system. $z = 0$ (vertical dashed line) denotes the central plane of the slit.

smaller than observed in bulk phenol. The state of adsorbed phenol molecules is strongly influenced by the heterogeneity of pore walls. The shapes of isobars simulated for ideal slits drastically differ from the data measured experimentally for studied carbon. The behavior of phenol in slit-like pores and in pores of studied carbon is also different, if one considers the

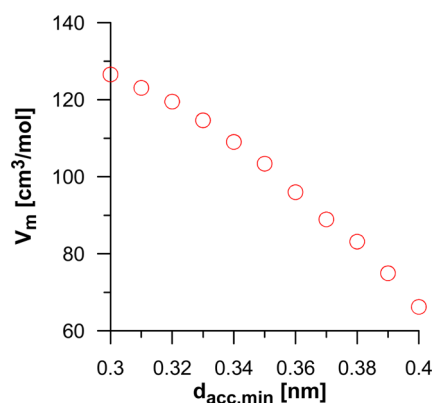


Figure 12. Molar volume of phenol adsorbed in the replica ($k = 1.7$) at $T = 301$ K calculated assuming different minimum effective diameters of accessible pores ($d_{acc,min}$) during volume integration.

RDF functions or the number of created hydrogen bonds, etc. Therefore, to obtain information on the properties of molecules in pores of heterogeneous adsorbents, it is necessary to construct reliable model of a solid using the most sophisticated methods.

Our results suggest that phenol adsorbed at ambient temperature in small carbon micropores forms a quasi-solid. This situation should be similar during adsorption from concentrated phenol solutions if H-type isotherms following the classification of Giles et al.²⁰ are observed.

■ ASSOCIATED CONTENT

■ Supporting Information

The Supporting Information is available free of charge on the ACS Publications website at DOI: 10.1021/acs.jpcc.5b06136.

Details of interaction energy calculations (PDF)

Animation_01: equilibrium configurations of phenol molecules adsorbed in the replica for $k = 1.7$ at different temperature; the view on the whole system along the slits and the views from the tops on the subsequent slits are shown (MPG)

Animation_02: comparison of phenol adsorption mechanism in the replica ($k = 1.7$) and the ideal slit-like systems for $H_{eff} = 0.4$ and 0.5 nm; the views on the whole systems along the slits and the views from the top on the middle slits are shown (MPG)

Animation_03: comparison of phenol adsorption mechanism in the ideal slit-like systems for $H_{eff} = 0.5, 0.6$, and 0.7 nm; the views on the whole systems along the slits and the views on the middle slits are shown; in addition, the molecules having the distance between their center of benzene ring and carbon atoms forming pore walls (the distance to the plane defined by the mass centers of C atoms, i.e., not effective one) larger than 0.45 nm (arbitrarily chosen value) are marked using cyan (MPG)

■ AUTHOR INFORMATION

Corresponding Author

*E-mail aterzyk@chem.uni.torun.pl (A.P.T.).

Notes

The authors declare no competing financial interest.

■ ACKNOWLEDGMENTS

The authors acknowledge the use of the computer cluster at Poznań Supercomputing and Networking Centre (Poznań, Poland) as well as the Information and Communication Technology Centre of the Nicolaus Copernicus University (Toruń, Poland).

■ REFERENCES

- (1) Fleege, J. W.; Carman, K. R.; Nisbet, R. M. Indirect effect of contaminants in aquatic ecosystem. *Sci. Total Environ.* **2003**, *317*, 207–233.
- (2) Aguilar, C.; Borrull, F.; Marcé, R. M. On-line and off-line solid-phase extraction with styrene-divinylbenzene-membrane extraction disks for determining pesticides in water by reversed-phase liquid chromatography-diode-array detection. *J. Chromatogr. A* **1996**, *754*, 77–84.
- (3) Brinkman, U. A. Th. On-line sample treatment for or via column liquid chromatography. *J. Chromatogr. A* **1994**, *665*, 217–231.
- (4) Ehrhardt, H. M.; Rehm, H. J. Phenol degradation by microorganisms adsorbed on activated carbon. *Appl. Microbiol. Biotechnol.* **1985**, *21*, 32–36.
- (5) Ehrhardt, H. M.; Rehm, H. J. Semicontinuous and continuous degradation of phenol by *Pseudomonas putida* P8 adsorbed on activated carbon. *Appl. Microbiol. Biotechnol.* **1989**, *30*, 312–317.
- (6) Annadurai, G.; Juang, R.-S.; Lee, D.-J. Biodegradation and adsorption of phenol using activated carbon immobilized with *Pseudomonas putida*. *J. Environ. Sci. Health, Part A: Toxic/Hazard. Subst. J. Environ. Sci. Health, Part A: Toxic/Hazard. Subst. Environ. Eng.* **2002**, *37*, 1133–1146.
- (7) Terzyk, A. P. Further insights into the role of carbon surface functionalities in the mechanism of phenol adsorption. *J. Colloid Interface Sci.* **2003**, *268*, 301–329.
- (8) Harris, P. J. F.; Burian, A.; Duber, S. High-resolution electron microscopy of a microporous carbon. *Philos. Mag. Lett.* **2000**, *80*, 381–386.
- (9) Harris, P. J. F. Fullerene-related structure of non-graphitizing carbons. In *Carbon Materials – Theory and Practice*; Terzyk, A. P., Gauden, P. A., Kowalczyk, P., Eds.; Research Signpost: Kerala, India, 2008; pp 1–14.
- (10) Harris, P. J. F. Fullerene-like models for microporous carbon. *J. Mater. Sci.* **2013**, *48*, S65–S77.
- (11) Pikunic, J.; Clinard, Ch.; Cohaut, N.; Gubbins, K. E.; Guet, J.-M.; Pellenq, R. J.-M.; Rannou, I.; Rouzaud, J.-N. Structural modeling of porous carbons: constrained reverse Monte Carlo method. *Langmuir* **2003**, *19*, 8565–8582.
- (12) Pikunic, J.; Llewellyn, P.; Pellenq, R. J.-M.; Gubbins, K. E. Argon and nitrogen adsorption in disordered nanoporous carbons: simulation and experiment. *Langmuir* **2005**, *21*, 4431–4440.
- (13) Jain, S. K.; Pellenq, R. J.-M.; Pikunic, J. P.; Gubbins, K. E. Molecular modeling of porous carbons using the hybrid reverse Monte Carlo method. *Langmuir* **2006**, *22*, 9942–9948.
- (14) Petersen, T. C.; Snook, I. K.; Yarovsky, I.; McCulloch, D. G.; O'Malley, B. Curved-surface atomic modeling of nanoporous carbon. *J. Phys. Chem. C* **2007**, *111*, 802–812.
- (15) Palmer, J. C.; Brennan, J. K.; Hurley, M. M.; Balboa, A.; Gubbins, K. E. Detailed structural model for activated carbons from molecular simulation. *Carbon* **2009**, *47*, 2904–2913.
- (16) Kowalczyk, P.; Terzyk, A. P.; Gauden, P. A.; Furmaniak, S.; Wiśniewski, M.; Burian, A.; Hawelek, L.; Kaneko, K.; Neimark, A. V. Carbon molecular sieves: reconstruction of atomistic structural models with experimental constraints. *J. Phys. Chem. C* **2014**, *118*, 12996–13007.
- (17) Terzyk, A. P.; Gauden, P. A.; Furmaniak, S.; Wesolowski, R. P.; Harris, P. J. F. Molecular dynamics simulation insight into the mechanism of phenol adsorption at low coverages from aqueous solutions on microporous carbons. *Phys. Chem. Chem. Phys.* **2010**, *12*, 812–817.

- (18) Terzyk, A. P.; Gauden, P. A.; Zieliński, W.; Furmaniak, S.; Wesolowski, R. P.; Klimek, K. K. First molecular dynamics simulation insight into the mechanism of organics adsorption from aqueous solutions on microporous carbons. *Chem. Phys. Lett.* **2011**, *515*, 102–108.
- (19) Gauden, P. A.; Terzyk, A. P.; Furmaniak, S.; Wloch, J.; Kowalczyk, P.; Zieliński, W. MD simulation of organics adsorption from aqueous solution in carbon slit-like pores. foundations of the pore blocking effect. *J. Phys.: Condens. Matter* **2014**, *26*, 055008.
- (20) Giles, C. H.; MacEwan, T. H.; Nakhwa, S. N.; Smith, D. Studies in adsorption. Part XI. A system of classification of solution adsorption isotherms, and its use in diagnosis of adsorption mechanisms and in measurement of specific surface areas of solids. *J. Chem. Soc.* **1960**, 3973–3993.
- (21) Gauden, P. A.; Terzyk, A. P.; Kowalczyk, P.; Aranovich, G. L.; Donohue, M. D.; Cwiertnia, M.; Furmaniak, S.; Rychlicki, G. Giles' classification of solute adsorption isotherms for binary non-electrolyte solutions via lattice DFT supported by experimental sorption data from aqueous solutions on carbonaceous materials. In *Carbon Materials – Theory and Practice*; Terzyk, A. P., Gauden, P. A., Kowalczyk, P., Eds.; Research Signpost: Kerala, India, 2008; pp 517–570.
- (22) Bertoncini, C.; Raffaelli, J.; Fassino, L.; Odetti, H. S.; Bottani, E. J. Phenol adsorption on porous and non-porous carbons. *Carbon* **2003**, *41*, 1101–1111.
- (23) Bertoncini, C.; Odetti, H.; Bottani, E. J. Computer simulation of phenol physisorption on graphite. *Langmuir* **2000**, *16*, 7457–7463.
- (24) Stoeckli, F.; Hugi-Cleary, D. On the mechanisms of phenol adsorption by carbons. *Russ. Chem. Bull.* **2001**, *50*, 2060–2063.
- (25) Zawadzki, J. Infrared spectroscopy in surface chemistry of carbons. *Chem. Phys. Carbon* **1989**, *21*, 147–380.
- (26) Zawadzki, J.; Wiśniewski, M. An infrared study of the behavior of SO₂ and NO_x over carbon and carbon-supported catalysts. *Catal. Today* **2007**, *119*, 213–218.
- (27) Wiśniewski, M. Mechanistic aspects of N₂O decomposition over carbon films and carbon-film-supported catalysts. *Catal. Lett.* **2014**, *144*, 633–638.
- (28) Terzyk, A. P.; Gauden, P. A.; Zawadzki, J.; Rychlicki, G.; Wiśniewski, M.; Kowalczyk, P. Toward the characterisation of microporosity of carbonaceous films. *J. Colloid Interface Sci.* **2001**, *243*, 183–192.
- (29) Zawadzki, J.; Wiśniewski, M. Adsorption and decomposition of NO on carbon and carbon-supported catalysts. *Carbon* **2002**, *40*, 119–124.
- (30) Bhattacharya, S.; Gubbins, K. E. Fast method for computing pore size distributions of model materials. *Langmuir* **2006**, *22*, 7726–7731.
- (31) Furmaniak, S. New virtual porous carbons based on carbon EDIP potential and Monte Carlo simulations. *Comput. Methods Sci. Technol.* **2013**, *19*, 47–57.
- (32) Humphrey, W.; Dalke, A.; Schulten, K. VMD: visual molecular dynamics. *J. Mol. Graphics* **1996**, *14*, 33–38.
- (33) Yan, Q.; de Pablo, J. J. Hyper-parallel tempering Monte Carlo: application to the Lennard-Jones fluid and the restricted primitive model. *J. Chem. Phys.* **1999**, *111*, 9509–9516.
- (34) Furmaniak, S.; Terzyk, A. P.; Gauden, P. A.; Kowalczyk, P.; Szymański, G. S. Influence of activated carbon surface oxygen functionalities on SO₂ physisorption – simulation and experiment. *Chem. Phys. Lett.* **2013**, *578*, 85–91.
- (35) Furmaniak, S. Influence of activated carbon porosity and surface oxygen functionalities' presence on adsorption of acetonitrile as a simple polar volatile organic compound. *Environ. Technol.* **2015**, *36*, 1984–1999.
- (36) Mooney, D. A.; Müller-Plathe, F.; Kremer, K. Simulation studies for liquid phenol: properties evaluated and tested over a range of temperatures. *Chem. Phys. Lett.* **1998**, *294*, 135–142.
- (37) Frenkel, D.; Smit, B. *Understanding Molecular Simulation*; Academic Press: San Diego, 1996.
- (38) Lau, K. F.; Alper, H. E.; Thacher, T. S.; Stouch, T. R. Effects of switching functions on the behavior of liquid water in molecular dynamics simulations. *J. Phys. Chem.* **1994**, *98*, 8785–8792.
- (39) Fennell, C. J.; Gezelter, D. Is the Ewald summation still necessary? Pairwise alternatives to the accepted standard for long-range electrostatics. *J. Chem. Phys.* **2006**, *124*, 234104.
- (40) Steele, W. A. *The Interaction of Gases with Solid Surfaces*; Pergamon Press: Oxford, UK, 1974.
- (41) Gordillo, M. C.; Martí, J. Hydrogen bond structure of liquid water confined in nanotubes. *Chem. Phys. Lett.* **2000**, *329*, 341–345.
- (42) Zawadzki, J. Infrared studies of aromatic compounds adsorbed on the surface of carbon films. *Carbon* **1988**, *26*, 603–611.
- (43) Wiśniewski, M.; Pacholczyk, A.; Terzyk, A. P.; Rychlicki, G. New phosphorus-containing spherical carbon adsorbents as promising materials in drug adsorption and release. *J. Colloid Interface Sci.* **2011**, *354*, 891–894.
- (44) Wiśniewski, M.; Terzyk, A. P.; Gauden, P. A.; Kaneko, K.; Hattori, Y. Y. Removal of internal caps during hydrothermal treatment of bamboo-like carbon nanotubes and application of tubes in phenol adsorption. *J. Colloid Interface Sci.* **2012**, *381*, 36–42.
- (45) Nguyen, T. X.; Bae, J.-S.; Wang, Y.; Bhatia, S. K. On the strength of the hydrogen-carbon interaction as deduced from physisorption. *Langmuir* **2009**, *25*, 4314–4319.